PERGAMON

Radiation Physics and Chemistry 56 (1999) 539–545

Radiation Physics and Chemistry

www.elsevier.com/locate/radphyschem

# EPR/ENDOR study of an X-irradiated single crystal of 1-triphenylphosphoranylidene-2-propanone: The role of hydrogen bonds in the trapping of radiogenic radicals

T. Berclaz[a], G. Bernardinelli[b], M. Geoffroy[a,*], G. Rao[a], Z. Tancic[a]

[a]*Department of Physical Chemistry, 30 Quai Ernest Ansermet, 1211, Geneva, Switzerland*
[b]*Laboratory of Crystallography, 30 Quai Ernest Ansermet, 1211, Geneva, Switzerland*

Received 5 January 1999; accepted 25 February 1999

**Abstract**

As shown from the crystal structure, the oxygen atom of $Ph_3P{=}CH{-}C(O)CH_3$ forms both intra and intermolecular hydrogen bonds. X-irradiation of this compounds produces a room-temperature-stable radical which was studied by single crystal EPR/ENDOR spectroscopy. Comparison of the experimental hyperfine couplings with those obtained from ab initio calculations shows that the radical cation $Ph_3P^+{-}CH{=}C(OH)CH_2$ is formed under radiolysis. The principal directions of the hyperfine tensors indicate that, in this process, some of the hydrogen bonds are broken and that the radical undergoes a drastic reorientation around the $Ph_3P{-}C$ bond. 

## 1. Introduction

The presence of intra- and intermolecular hydrogen bonding can considerably influence the nature and the structure of radiation damage. In particular, the radiolytic scission of these bonds can induce drastic local changes in the molecular geometry and provoke internal reorientations . Information on this process can be obtained by studying the structure of a radiogenic radical localized on the molecular moiety involving hydrogen bonds. In the present paper, we endeavour to identify the radiation effects on an organophosphorus moiety whose orientations in the original molecule and in the molecular packing result from hydrogen bond interactions. This study is therefore composed of the three following points: (i) X-ray diffraction study of (**1**) to get evidence on hydrogen bonding; (ii) EPR/ENDOR study of an X-irradiated single crystal of (**1**) to characterise the radiation damage; (iii) Quantum mechanical calculations to identify the trapped radical.

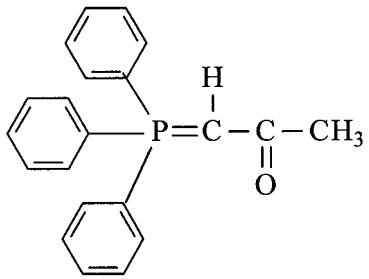


* Corresponding author at: Université de Genève, Department of Chimie Physique, 30 Quai Ernest-Ansermet, 1211 Geneva 4, Switzerland. Tel.: +22-702-65-52; fax: +22-702-61-03.

*E-mail address:* Michel.Geoffroy@chiphy.unige.ch (M. Geoffroy)

0969-806X/99/$ - see front matter 
PII: S0969-806X(99)00295-9

## 2. Experimental

### 2.1. Compound

1-Triphenylphosphoranylidene-2-propanone (**1**) is a commercial product (Aldrich) which was purified by recrystallisation in $CH_2Cl_2$. $(C_6D_5)_3P{=}C(H)C(O)CH_3$ was synthesized using $C_6D_5Br$ as a precursor and by following an already described method (Ramirez and Derhowitz, 1957).

### 2.2. Crystal structure determination[1]

Crystals of $C_{21}H_{19}OP$ (**1**) were obtained from solutions in $CH_2Cl_2$. The cell parameters and intensities were measured at room temperature on a Nonius CAD4 diffractometer with graphite-monochromated Mo[K$\alpha$] radiation ($\lambda = 0.71069$ Å), $\omega$–$2\theta$ scans, scan width $1.2° + 0.25$ tg $\theta$, and scan speed 0.02–0.14°/s. Two reference reflections measured every 60 min showed no variation. Data were corrected for Lorentz and polarization effects but not for absorption. The structure was solved by direct methods using MULTAN 87 (Main et al., 1987), all other calculations used XTAL system (Hall et al., 1992) and ORTEP (Johnson, 1976) programs. Hydrogen atoms of the —$CH_3$ group were placed in calculated positions and the others were observed and refined with a fixed value of isotropic displacement parameters ($U = 0.05$ Å$^2$).

### 2.3. Irradiation and EPR/ENDOR

Large single crystals of (**1**) (3 × 2 × 2 mm) were grown by slow evaporation in $CH_2Cl_2$; their faces were indexed and an EPR/ENDOR reference frame was determined in such a way that the *ox, oy, oz* axes are aligned along the *c*, $-a^*$ and $-b$ crystallographic axis respectively. The crystals were irradiated for 3 h at room temperature with a Philips X-ray tube (tungsten anticathode, 30 mA, 30 kV). The EPR spectra were recorded at 300 K on a Bruker 200 spectrometer (X-band, 100 kHz magnetic field modulation). The ENDOR spectra were measured at 200 K with a homemade device: the single crystal was oriented in a two-loop copper coil, the radio frequency was produced by a Waveteck frequency generator and the rf power (ENI model 3100) was dissipated in a 50 Ω resistor. ENDOR and EPR studies were performed by measuring the spectra by steps of 10° in the reference planes *xyz*. Simulations of the EPR spectra were carried out by using a homemade program which uses a spin Hamiltonian containing electronic and nuclear Zeemann terms as well as the various hyperfine contributions, the positions of the transitions are calculated with second order perturbation theory.

Table 1
Summary of crystal data, intensity measurement and structure refinement for **1**

| | |
|---|---|
| Formula | $C_{21}H_{19}OP$ |
| Mol. wt | 318.4 |
| Crystal size (mm) | $0.20 \times 0.22 \times 0.25$ |
| Crystal system | Monoclinic |
| Space group | $P\,2_1/n$ |
| a (Å) | 8.8680(7) |
| b (Å) | 19.3853(11) |
| c (Å) | 10.4724(9) |
| $\beta$ (°) | 94.374(5) |
| $V$ (Å$^3$) | 1795.1(2) |
| $Z$ | 4 |
| $F(000)$ | 672 |
| Dc (gr cm$^{-3}$) | 1.178 |
| $\mu$(MoK$\alpha$) (mm$^{-1}$) | 0.150 |
| $((\sin\theta)/\lambda)_{max}$ (Å$^{-1}$) | 0.53 |
| Temperature (K) | 298 |
| No. measured refl. | 2457 |
| No. observed refl. | 1737 |
| $R_{int}$ for equiv. Refl. | 0.014 |
| Criterion for observed | $\|Fo\| > 4\sigma(Fo)$ |
| Refinement (on $F$) | Full-matrix |
| No. parameters | 256 |
| Weighting scheme | $\omega = 1/\sigma^2(Fo)$ |
| Max. $\Delta/\sigma$ | 0.065 |
| Max. and min. $\Delta\rho$(e.Å$^{-3}$) | 0.38, −0.50 |
| $S$[a] | 2.34 |
| $R$[b], $\omega R$[c] | 0.058, 0.041 |

[a] $S = [\Sigma\{((Fo–Fc)/\sigma(Fo))^2\}/(N_{ref}–N_{var})]^{1/2}$.
[b] $R = \Sigma\|\|Fo|–|Fc\|/\Sigma|Fo|$.
[c] $\omega R = [\Sigma(\omega|Fo|–|Fc|)^2/\Sigma\omega|Fo|^2]^{1/2}$.

### 2.4. Calculations

Ab initio calculations were performed with the Gaussian 94 package (Frisch et al., 1995). UHF calculations were carried out with a 6–31G* basis set. Spin densities, Fermi contact and magnetic dipolar interactions were calculated after annihilation of the spin contamination.

## 3. Results

### 3.1. Crystal structure

A summary of crystal data is given in Table 1 while

[1] Crystallographic data (excluding structure factors) have been deposited to the Cambridge Crystallographic Data Base (deposition No. 111491). Copies of the data can be obtained free of charge on application to the CCDC, 12 Union Road, Cambridge CB2 1EZ, UK (fax: Int. + 44 (1223) 336-033; e-mail: deposit@ccdc.cam.ac.uk).

Table 2
Selected bond lengths (Å), bond angles and torsional angles (°) for **1**

| | | | |
|---|---|---|---|
| P-C1 | 1.710(5) | O-C2 | 1.247(6) |
| P-C4 | 1.811(4) | C1-C2 | 1.391(7) |
| P-C10 | 1.801(4) | C2-C3 | 1.520(7) |
| P-C16 | 1.801(4) | | |
| C1-P-C4 | 116.5(2) | C10-P-C16 | 107.2(2) |
| C1-P-C10 | 107.3(2) | P-C1-C2 | 119.6(4) |
| C1-P-C16 | 112.7(2) | O-C2-C1 | 122.9(4) |
| C4-P-C10 | 106.0(2) | O-C2-C3 | 118.6(4) |
| C4-P-C16 | 106.6(2) | C1-C2-C3 | 118.5(4) |
| C4-P-C1-C2 | 74.4(4) | C1-P-C4-C5 | 134.2(4) |
| C10-P-C1-C2 | −167.1(4) | P-C1-C2-O | −5.2(6) |
| C16-P-C1-C2 | −49.4(4) | P-C1-C2-C3 | 173.2(3) |
| Hydrogen bonds | | | |
| Intra: C9…O = 3.182(6) Å | | H9…O = 2.37(4) Å | |
| C9—H9…O = 146(3)° | | | |
| Inter: C20…O[a] = 3.181(6) Å | | H20…O[a] = 2.39(4) Å | |
| C20—H20…O[a] = 137(3)° | | | |
| Inter: C13…O[b]) = 3.309(7) Å | | H13…0[b] = 2.36(4) Å | |
| C13—H13…O[b] = 166(3)° | | | |

[a] Equivalent position: $1/2+x$, $3/2-y$, $1/2+z$.
[b] 3/2−i x, $y-1/2$, $1/2-z$.

selected geometrical parameters are reported in Table 2. A perspective view of the crystal structure is given in Fig. 1. While the P—$C_{(1)}$ (1.710(5) Å) and $C_{(2)}$—O (1.247(6) Å) bonds are significantly longer than common corresponding double bonds (P=C in $Ph_3P{=}CH_2$: 1.66 Å, C=O in $CH_3C(H)O$: 1.215 Å), the $C_{(1)}$—C(2) bond (1.391(7) Å) is shorter than a simple C—C bond (C—C in $C_2H_6$: 1.534 Å). These bond lengths indicate a large contribution of the mesomeric form **b**.

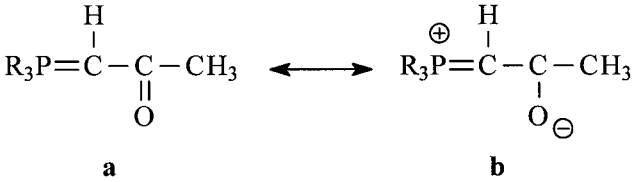


**a** **b**

An important point, in the context of the present study, is the presence of intra- and intermolecular hydrogen bonds (Fig. 2) (Desiraju, 1996; Steiner, 1997). Thus, the oxygen is involved as acceptor in a trifurcated hydrogen bond interaction. One intramolecular C—H…O hydrogen bond precludes the rotation

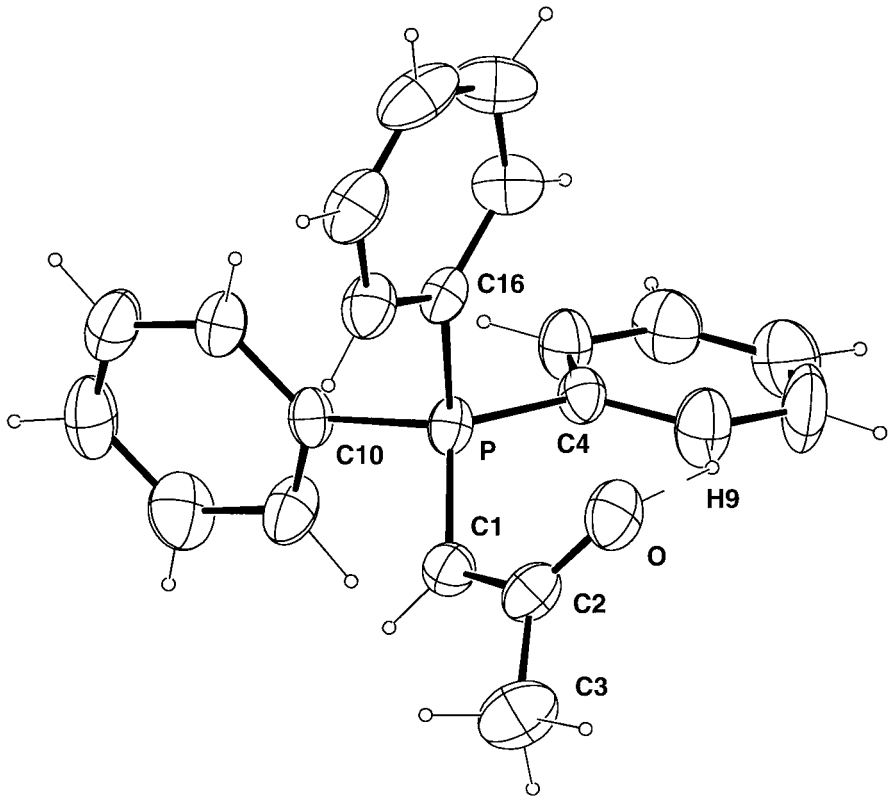


Fig. 1. Perspective view of the crystal structure of **1** showing the intramolecular hydrogen bond. Ellipsoids are represented with 40% probability level.

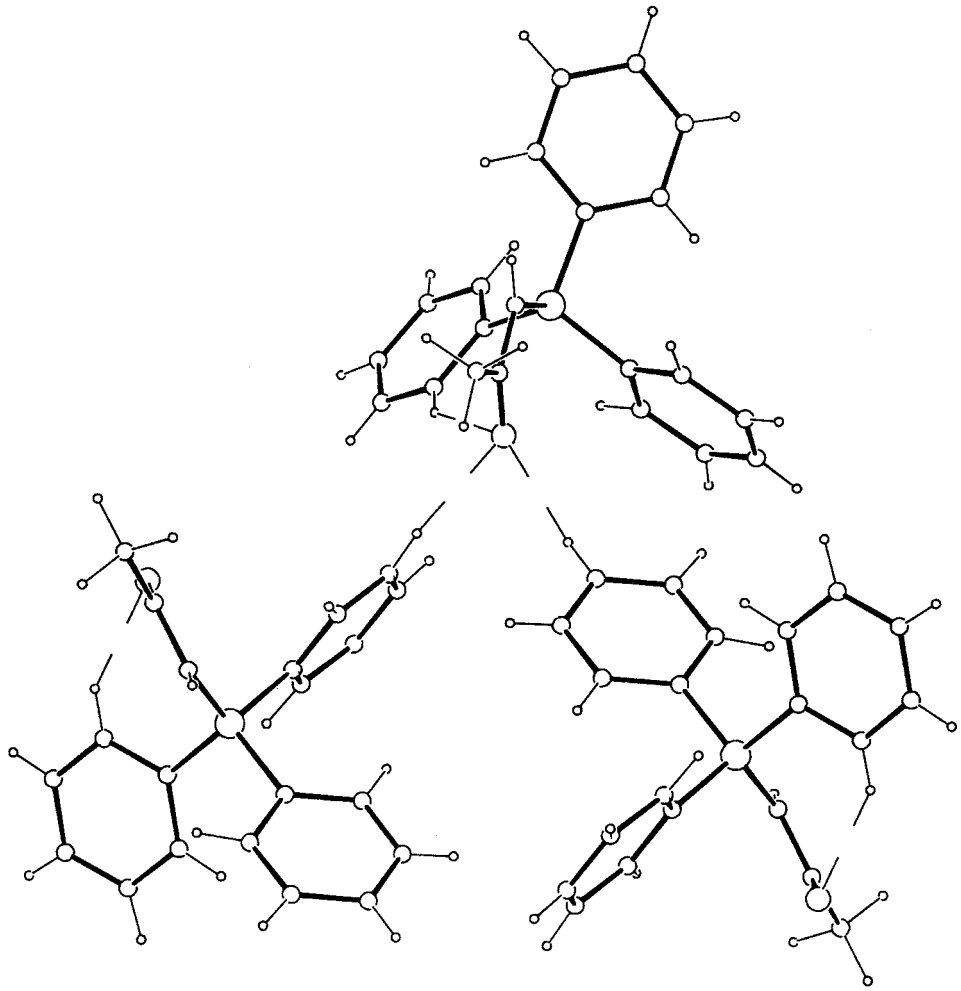

Fig. 2. Perspective view of the crystal structure of **1** showing the inter and intramolecular hydrogen bond network.

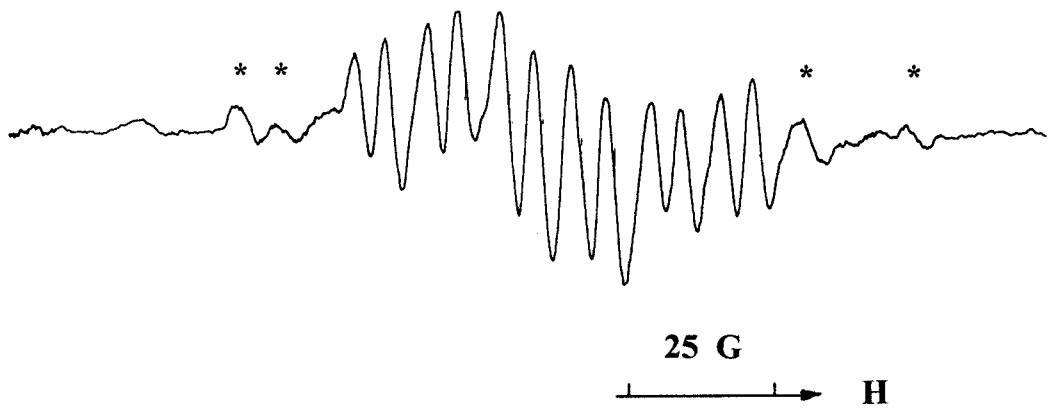


Fig. 3. Example of an EPR spectrum obtained with an X-irradiated single crystal of **1**. The lines marked ∗ correspond to an unidentified radical and have not been considered in this study.

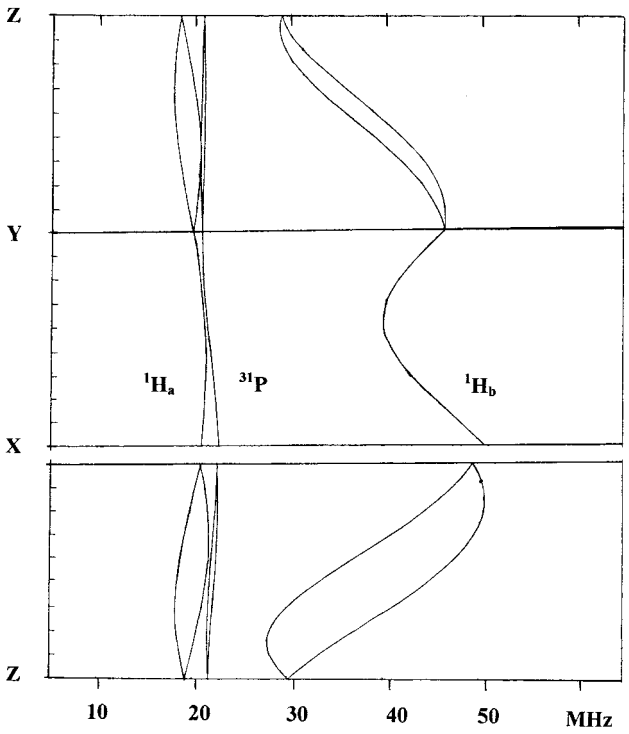


Fig. 4. Angular variation of the ENDOR signals obtained with an X-irradiated single crystal of **1**. The duplication of the lines in the *xz* and *yz* planes is due to two magnetically non-equivalent orientations of the radical.

of the $C_{(4)}$—$C_{(9)}$ phenyl group and two C—H...O intermolecular interactions with neighbouring molecules participate in the rigidity of the molecular packing (see Table 2). It should be noted that the intramolecular hydrogen interaction could be at the origin of the non-planar distribution of the P═C—C═O fragment (torsional angle P═$C_{(1)}$—$C_{(2)}$═O: −5.2(6)°). No stacking interaction is observed in the molecular packing.

### 3.2. EPR and ENDOR spectroscopies

An example of an EPR spectrum obtained with an X-irradiated single crystal of **1** is shown in Fig. 3. The fact that the hyperfine structure of this spectrum is not affected by deuteration of the phenyl rings rules out the trapping of the cyclohexadienyl radical which could be formed by addition of an hydrogen atom on a benzene ring. Due to the complexity of the spectra, the angular dependence of the EPR signals could not be directly followed. We tried therefore to measure hyperfine couplings from ENDOR spectra (Kevan and Kispert, 1976). ENDOR spectra obtained at 200 K clearly show signals due to two magnetically distinct protons ($H_a$ and $H_b$) and one $^{31}P$ nucleus. In accord with the crystal structure, the angular variations of these signals show that, in the planes *xz* and *zy*, the radical species is trapped along two magnetically non-

Table 3
Experimental EPR tensors

| | | Eigenvectors | | |
|---|---|---|---|---|
| Tensor | Eigenvalues (MHz) | $\lambda$ | $\mu$ | $\nu$ |
| g[a] | 2.0018 | | | |
| | 2.0021 | | | |
| | 2.0030 | | | |
| $^{31}P$–T[b] | 29.5 | −0.1453 | 0.8749 | ±0.4620 |
| | 30.5 | −0.1610 | −0.4816 | ±0.8615 |
| | 32.8 | 0.9762 | 0.0508 | ±0.2108 |
| $^1H_a$–T[b] | −7.1 | 0.3680 | 0.3384 | ±0.8668 |
| | −11.2 | −0.6112 | 0.7901 | ∓0.0471 |
| | −16.3 | 0.7007 | 0.5125 | ∓0.4964 |
| $^1H_b$–T[b] | −23.8 | 0.3267 | −0.2345 | ±0.9157 |
| | −54.8 | −0.5133 | 0.7695 | ±0.3799 |
| | −83.0 | 0.7936 | 0.5942 | ∓0.1313 |
| $^1H_c$–T[a] | −46.1 | | | |
| | −56.1 | | | |
| | −80.1 | | | |

[a] Determined from simulation of the EPR spectra.
[b] Determined from ENDOR measurements.

Table 4
Ab initio calculated hyperfine couplings for the neutral radical $H_3P{=}C(H){-}C(O)CH_2$ and the radical cation $H_3P^+{-}CH{=}C(OH)CH_2$

| | $A_{iso}$ (MHz) | | Anisotropic coupling (MHz) | | | | | |
|---|---|---|---|---|---|---|---|---|
| | Neutral | Cation | Neutral | | | Cation | | |
| Coupling | | | $\tau_1$ | $\tau_2$ | $\tau_3$ | $\tau_1$ | $\tau_2$ | $\tau_3$ |
| $^{31}P$ | 1.4 | −41.4 | −0.82 | +0.45 | +1.3 | −1.9 | +0.7 | +1.2 |
| $^1H$ ($C_1$–H) | −1.8 | −17.8 | −1.87 | −1.7 | +3.5 | −5.6 | −3.1 | +8.8 |
| $^1H$ ($C_3$-H) | −39.3 | −36.6 | −33.6 | −1.9 | +35.7 | −28.5 | −2.7 | +31.2 |
| $^1H$ ($C_3$–H) | −40.6 | −37.5 | −32 | −1.9 | +32 | −29.3 | −2 | +30.9 |
| $^1H$ (O–H) | | −0.5 | | | | −1.98 | −1.0 | +3 |

equivalent orientations. The analysis of these curves (Fig. 4) leads to the hyperfine tensors $^{31}P$—T, $^1H_a$—T and $^1H_b$—T given in Table 3. Using these tensors to simulate the EPR spectra shows that an additional coupling with a spin 1/2 nucleus must be taken into account to reproduce these spectra. Our attempts to clearly detect the corresponding ENDOR signals remained unsuccessful. Nevertheless, by simulating all the EPR spectra, with the help of the ENDOR couplings, we could estimate this additional hyperfine tensor as well as the *g*-tensor. The accuracy of these two latter tensors is, of course, considerably less than for the other couplings and we will not consider their eigenvectors for the discussion; the corresponding eigenvalues are also given in Table 3.

### 3.3. Ab initio calculations

Radicals directly generated from **1** are too large to be directly investigated by ab initio methods. We have therefore studied radicals where phenyl rings have been replaced by hydrogen atoms. The objective of these calculations is to know to what extent the hyperfine couplings allow differentiation between the neutral radical $H_3P{=}CH{-}C(O)CH_2$ and the positively charged species $H_3P^+{-}CH{=}C(OH)CH_2$.

The optimized geometries show that in the neutral structure the $H_3P$—C bond length is equal to 1.679 Å while this same bond increases to 1.762 Å in the species bearing a phosphonium group. Fermi contact interaction and dipolar couplings have been calculated for these two species after annihilation of the spin contamination (final $\langle S^2\rangle$ values equal to 0.751 and 0.753). The resulting parameters are given in Table 4. They show that the main differences between the two species lie in the absolute values of the $^{31}P$ and $^1H(C_{(1)}{-}H)$ isotropic constants which are appreciably larger for the cation.

Table 5
Experimental isotropic and anisotropic coupling constants

| Nucleus | Isotropic couplings (MHz) | Anisotropic couplings (MHz) | | |
|---|---|---|---|---|
| $^{31}P$ | ∓30.9 | ∓1.9 | ±0.4 | ±1.4 |
| $^1Ha$ | ∓11.5 | ∓4.8 | ±0.3 | ±4.4 |
| $^1Hb$ | ∓53.8 | ∓29.2 | ±1 | ±30.2 |
| $^1Hc$ | ∓60.7 | ∓19.4 | ±4.6 | ±14.6 |

## 4. Discussion

The various experimental isotropic and anisotropic coupling constants, obtained by assuming that for each coupling the three eigenvalues have the same sign, are given in Table 5.

Comparison with the atomic coupling constants ($A_{iso}=13{,}306$ MHz, $2B_0=730$ MHz (Morton and Preston, 1978)) shows that the delocalization of the unpaired electron on the phosphorus atom is very low ($\rho_s(P)=0.002$, $\rho_p(P)=0.002$) and indicates that there is no participation of a phosphoranyl moiety to the structure of the trapped radical. An electron capture by *b* to give $R_3P^{\cdot}{-}C(H){=}C(O^-){-}CH_3$ can therefore

Table 6
Orientation of the radical as given by the hyperfine eigenvectors

| Angle[a] | Site 1 |
|---|---|
| *n*, $p_\pi(C1)$ | 81° |
| *n*, $p_\pi(C2)$ | 83° |
| $(C_1{-}H)_{endor}$, $(C_1{-}H)_{crystal}$ | 95° |
| $p_\pi(C_1)$, $p_\pi(C_2)$ | 20° |

[a] *n*: normal to the crystallographic CPC1C2 plane. $p_\pi$ direction of the $\pi$ orbital as given by the intermediate dipolar coupling $\tau$ of the $\alpha$ proton determined from ENDOR measurement.

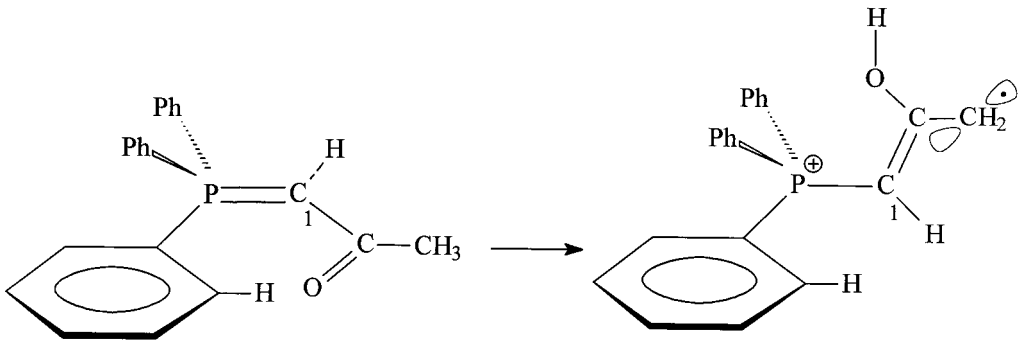


Scheme. 1

be ruled out. At first sight the presence of a small $^{31}P$ coupling together with three $^{1}H$ couplings suggests the formation of $R_3P{=}CH{-}C(O){-}CH_2$. The calculated dipolar eigenvalues reported in Table 4 for the model radical $H_3P{=}CH{-}C(O){-}CH_2$ are not in conflict with this identification; however, the calculated spin density on the $C_{(1)}$ carbon seems to be quite smaller than the experimental one (spin density from gross orbital spin populations: 2%, experimental spin density from the McConnell relation = 16%). A more serious discrepancy is revealed by the orientation of the eigenvectors: in $H_3P{=}CH{-}C(O){-}CH_2$ the $C_{(1)}{-}H_{(1)}$ bond lies in the molecular plane, whereas the experimental direction cosines (Table 5 and 6) indicate that the $C_{(1)}$—H bond is perpendicular to the crystallographic $PC_{(1)}C_{(2)}$ plane.

Therefore, a drastic change in the conformation of the phosphinylidene molecule probably occurs under radiolysis. This suggests that after ionization of **1**, the unstable cation $R_3P^+{-}CH{=}C(0^{\cdot}){-}CH_3$ gives rise to $R_3P^+{-}CH{=}C(0H){-}^{\cdot}CH_2$. In this process (Scheme 1) the original hydrogen bond between the phenyl and the carbonyl groups is broken, the length of the phosphorus–carbon bond (which becomes a single bond) increases, the rotation barrier around this bond decreases and the CH—C(OH)—$CH_2$ moiety rotates around this P—$C_1$ bond. It is probable that this reorientation is accompanied by a scission of the intermolecular hydrogen bonds.

As shown in Table 6 the eigenvalues calculated for $H_3P^+{-}CH{=}C(OH)CH_2$ are consistent with the experimental ones, in particular the isotropic couplings with $^{31}P$ and the proton of the $C_{(1)}H$ bond. A slight distortion of the model molecule (rotation of the $CH_2$ group around the C(OH)—$CH_2$ bond is however required to reproduce the experimental ($p_\pi(C_{(1)})$, $p_\pi(C_{(2)})$) of 20°. It is probable that interaction between the damaged molecule and a neighbour molecule hinders a free reorientation of the $C{=}C(OH)CH_2$ moiety and that the intermolecular bonds are involved in this distortion.

## References

Desiraju, G.R., 1996. The C—H...O hydrogen bond: structural implications and supramolecular design. Acc. Chem. Res 29, 441–449.

Frisch, M.J., Trucks, G.W., Schlegel, H.B., Gill, P.M.W., Johnson, B.G., Robb, M.A., Cheeseman, J.R., Keith, T., Petersson, G.A., Montgomery, J.A., RaghavacHari, K., Al-Laham, M.A., Zakrzewski, V.G., Ortiz, J.V., Foresman, J.B., Ciolowski, J., Stefanov, B.B., Nanayakkara, A., Challacombe, M., Peng, C.Y., Ayala, P.Y., Chen, W., Wong, M.W., Andres, J.L., Replogle, E.S., Gomperts, R., Martin, R.L., Fox, D.J., Binkley, J.S., Defrees, D.J., Baker, J., Stewart, J.P., Head-Gordon, M., Gonzalez, C., Pople, J., 1995. Gaussian 94, Revision B.1. Gaussian Inc, Pittsburgh, PA.

Hall, S.R., Flack, H.D., Stewart, J.M., 1992. Eds XTAL3.2 User's Manual. Universities of, Western Australia and Maryland.

Johnson, C.K., 1976. ORTEP II, Report ORNL-5138. Oak Ridge National Laboratory: Oak Ridge, TN.

Kevan, L., Kispert, L.D., 1976. Electron Spin Double Resonance Spectroscopy. John Wiley, New York.

Main, P., Fiske, S.J., Hull, S.E., Lessinger, L., Germain, G., Declercq, J-P., Woolfson, M.M., 1987. A System of Computer Programs for the Automatic Solution of Crystal Structures from X-Ray Diffraction Data. Universities of, York, England, and Louvain-la-Neuve, Belgium.

Morton, J.R., Preston, K.F.J., 1978. Atomic parameters for paramagnetic resonance data. Magn. Reson 30, 577.

Ramirez, F., Derhowitz, S., 1957. Phosphinemethylenes. II. Triphenylphosphineacyl methylenes. J. Org. Chem 22, 41–45.

Steiner, T.J., 1997 Unrolling the hydrogen bond properties of C—H...O interactions, Chem. Commun 727–734.